

Influence of Coulomb and Phonon Interaction on the Exciton Formation Dynamics in Semiconductor Heterostructures

Walter Hoyer,¹ Mackillo Kira,¹ and Stephan W. Koch¹

¹Department of Physics and Material Sciences Center,
Philipps University, Renthof 5, D-35032 Marburg, Germany
(dated: March 22, 2024)

A microscopic theory is developed to analyze the dynamics of exciton formation out of incoherent carriers in semiconductor heterostructures. The carrier Coulomb and phonon interaction is included consistently. A cluster expansion method is used to systematically truncate the hierarchy problem. By including all correlations up to the four-point (i.e. two-particle) level, the fundamental fermionic substructure of excitons is fully included. The analysis shows that the exciton formation is an intricate process where Coulomb correlations rapidly build up on a picosecond time scale while phonon dynamics leads to true exciton formation on a slow nanosecond time scale.

PACS numbers: 71.35.-y, 71.10.-w, 73.21.Hb

Keywords: exciton formation, many-body correlations

I. INTRODUCTION

The linear absorption spectrum of an intrinsic direct-gap semiconductor in its ground state shows excitonic resonances energetically below the fundamental band-gap energy. These resonances in the linear optical polarization are a consequence of the attractive Coulomb interaction between a conduction-band electron and a valence-band hole. Mathematically, the eigenvalue problem of an exciton in the so-called Wannier limit is identical to that of the hydrogen atom, such that all relevant properties are well known.¹

However, the appearance of excitonic signatures in optical spectra does not necessarily imply the population of excitonic states. Even if the optical excitation is directly resonant with the exciton energy, the optical excitation always induces optical polarization in the semiconductor. This polarization, respectively the absolute square of the polarization, is sometimes related to coherent populations; however, it does not yield information about the truly incoherent population of single particle or pair states.

Furthermore, the optically induced polarization and the other coherences decay away typically on a picosecond time scale due to: i) excitation-induced dephasing resulting from the carrier-carrier Coulomb scattering^{2,3}, ii) phonon scattering^{1,4,5}, and iii) the finite radiative lifetime^{6,7,8} in confined semiconductor structures. However, after the disappearance of the optical polarization the material is typically not back in its ground state since carrier densities and incoherent correlations remain in the system and continue their many-body dynamics for several nanoseconds. The lifetime of these incoherent excitations is limited only by slow radiative and non-radiative recombination processes. In ideal semiconductors, only spontaneous recombination determines the ultimate lifetime of the excited charge carriers.

In this context, an old but still open question concerns the nature of the incoherent Coulomb correlated populations, in particular the conditions under which a significant part of the electron-hole excitations exist in the form of bound pairs, i.e. Wannier excitons. Although it is not even clear a priori how to count bound states since a rigorous exciton number operator does not exist⁹, one wants to understand the quantum statistical properties of incoherent excitons, their distribution function, and possible bosonic as well as Bose condensation aspects.^{10,11}

So far, several papers discuss the relaxation dynamics of excitons due to phonons together with a direct bosonic approximation for the exciton^{12,13}. In other approaches, exciton formation after coherent excitation has been investigated, however, restricting the treatment to weak excitation conditions due to a low-order expansion in terms of the exciting pulse.^{14,15} Since these approaches do not involve fermionic carrier densities and carrier-carrier correlations, they cannot resolve how much of the excitation is transferred directly into those correlations and densities. Typically, in bosonic models, exciton contributions are separated into bound and continuum excitons. In this description, one cannot determine the plasma carrier density since the continuum excitons determined from the two-particle reduced density matrix are not trivially related to the carrier densities given by the one-particle reduced density matrix.

In this paper, we present and utilize a microscopic theory for the description of the totally incoherent regime. In this approach, fermionic carriers, incoherent exciton populations, carrier-carrier correlations, as well as phonon-assisted correlations are treated at the same level. As a result, we are able to evaluate the excitonic correlations, formation rates, distribution functions, etc. for different temperatures and carrier densities without neglecting the underlying fermionic anti-symmetry.

After presenting the theoretical background and the full equations in the incoherent limit in Sec. II, we discuss our numerical results in Sec. III. This is done by viewing the build-up of correlations and monitoring the growth of the

electron-hole pair-correlation function. We investigate the issue of energy conservation and derive an approximate adiabatic solution which offers the possibility to obtain an intuitive interpretation of the exciton formation process. The results are summarized in Sec. IV and some technical details of the calculations are presented in the appendices.

II. INCOHERENT EXCITON AND PLASMA DYNAMICS

In contrast to earlier investigations of exciton formation after resonant excitation^{14,15}, we focus in this paper on an initially completely incoherent con guration. Such a situation can be realized experimentally either by pulsed continuum excitation, after the initial coherences have decayed, or with a current injection of carriers since this process does not induce optical coherences. In all numerical investigations in this paper, we therefore start with vanishing correlations and finite carrier densities and view the evolution of the system developing from that initial condition.

A. The Hamiltonian

The starting point of our theoretical description is the full Hamiltonian which describes the free motion of non-interacting carriers and phonons as well as the interaction between those quasi-particles. In this section, we briefly outline the Hamiltonian which is used throughout the paper; for more detailed derivations, see e.g. Refs.^{1,16}.

In semiconductor heterostructures, the microscopic properties of the carriers can be described with the fermionic field operator $a_{\mathbf{k}}$ ($a_{\mathbf{k}}^\dagger$) annihilating (creating) an electron in band \mathbf{k} with wave vector \mathbf{k} along the heterostructure. Here, in general, the band index \mathbf{k} may include different bands, subbands, and spins. For sufficiently narrow confinement, the carrier dynamics is restricted practically completely to the lowest subband and the Bloch functions follow from the envelope approximation.¹ The corresponding free Hamiltonian is

$$H_{\text{kin}} = \sum_{\mathbf{k}} \left(\epsilon_{\mathbf{k}}^c a_{c;\mathbf{k}}^\dagger a_{c;\mathbf{k}} + \epsilon_{\mathbf{k}}^v a_{v;\mathbf{k}}^\dagger a_{v;\mathbf{k}} \right); \quad (1)$$

which includes one valence and one conduction band. The generalization to a multiband system or the inclusion of spin is straight forward.^{1,17} In general, the eigenenergies $\epsilon_{\mathbf{k}}^{c=v}$ must be obtained from precise band structure calculations. For the investigation of near-bandgap optical features, we may use $\epsilon_{\mathbf{k}}^c = \epsilon_{\mathbf{k}}^v + E_G = \frac{\hbar^2 k^2}{2m^e} + E_G$ and $\epsilon_{\mathbf{k}}^v = \epsilon_{\mathbf{k}}^h = \frac{\hbar^2 k^2}{2m^h}$ where m^e and m^h are the effective electron and hole masses. The unrenormalized bandgap is denoted with E_G .

In order to include the Coulomb interaction between the electrons in different bands, we use the Hamiltonian^{1,18}

$$H_C = \frac{1}{2} \sum_{\mathbf{k}, \mathbf{k}^0, \mathbf{q} \in 0} V_{\mathbf{q}} \left(a_{c;\mathbf{k}}^\dagger a_{c;\mathbf{k}^0}^\dagger a_{c;\mathbf{k}^0+\mathbf{q}} a_{c;\mathbf{k}-\mathbf{q}} + a_{v;\mathbf{k}}^\dagger a_{v;\mathbf{k}^0}^\dagger a_{v;\mathbf{k}^0+\mathbf{q}} a_{v;\mathbf{k}-\mathbf{q}} + 2 a_{c;\mathbf{k}}^\dagger a_{v;\mathbf{k}^0}^\dagger a_{v;\mathbf{k}^0+\mathbf{q}} a_{c;\mathbf{k}-\mathbf{q}} \right); \quad (2)$$

where $V_{\mathbf{q}}$ is the quantum-well or quantum-wire Coulomb matrix element. The first two terms in Eq. (2) lead to repulsive interaction between electrons within the same band whereas the last term gives rise to the attractive interaction between electrons and holes (missing valence band electrons) in different bands.

In semiconductors, the carriers are additionally coupled to lattice vibrations (phonons). The noninteracting part of the phonon Hamiltonian is

$$H_{\text{phon}} = \sum_{\mathbf{p}} \hbar \omega_{\mathbf{p}} \left(D_{\mathbf{p}}^\dagger D_{\mathbf{p}} + \frac{1}{2} \right); \quad (3)$$

where the bosonic operator $D_{\mathbf{p}}$ ($D_{\mathbf{p}}^\dagger$) annihilates (creates) a phonon in the state \mathbf{p} . Here, $\mathbf{p} = (\mathbf{p}_\parallel; \mathbf{p}_\perp; \lambda)$ labels the wave vector along and perpendicular to the heterostructure as well as the phonon branch. Corresponding to the three independent modes of sound waves in a solid, three branches of acoustic phonons always exist in a three-dimensional semiconductor.¹⁹ In lattices with more than one atom within a unit cell, additional optical phonon branches are present.

The carrier-phonon interaction Hamiltonian can be expressed in the form

$$H_P = \sum_{\mathbf{p}, \mathbf{p}'; \mathbf{k}} D_{\mathbf{p}; \mathbf{p}'}^\dagger \left(G_{\mathbf{p}; \mathbf{p}'}^c a_{c;\mathbf{k}}^\dagger a_{c;\mathbf{k}+\mathbf{p}} + G_{\mathbf{p}; \mathbf{p}'}^v a_{v;\mathbf{k}}^\dagger a_{v;\mathbf{k}+\mathbf{p}} \right) + \text{h.c.}; \quad (4)$$

where $G_{\mathbf{p}; \mathbf{p}'}$ is the effective coupling matrix element between a phonon and an electron in band \mathbf{k} . Only the momentum component p along the heterostructure is conserved because the Bloch electrons are confined in perpendicular direction

p_z . The form of Eq. (4) reflects the fact that phonon interaction takes place within one band because phonons cannot provide the energy for an interband transition. The exact form of the interaction matrix element $G_{p,p_z}^{c(v)}$ depends on the interaction type which is included (i.e. deformation potential, piezo-electric coupling, etc.). For the treatment of acoustic phonons in the long-wavelength limit, the matrix element is given by a product between the plain matrix element $C_p = \frac{\hbar p_z^2 p_z}{2V c_{LA}}$, where ρ denotes the mass density and V the volume of the semiconductor material, c_{LA} is the velocity of sound and D the deformation constant, and the form factor $f_R(p_z)$ which is a consequence of the confinement of the electrons in the direction perpendicular to the semiconductor structure. By choosing parabolic confinement, we obtain $f_R(p_z) = e^{-\frac{p_z^2 R^2}{2}}$ for a one-dimensional quantum wire characterized by the confinement potential $\frac{\hbar^2 x^2}{2m R^4}$.

The starting point of all our further investigations is the total Hamiltonian of Eq. (1)-(4),

$$H_{\text{tot}} = H_{\text{kin}} + H_C + H_{\text{phon}} + H_P; \quad (5)$$

where both interaction parts of the total Hamiltonian lead to non-trivial coupling to higher order correlations.

B. Hierarchy Problem

Starting from Eq. (5), one can use the Heisenberg equation to compute the equations of motion for all relevant expectation values of interest. The simplest examples of incoherent one-particle expectation values are the two-point quantities describing the electron and hole distributions

$$f_k^e = \langle a_{c,k}^\dagger a_{c,k} \rangle; \quad f_k^h = \langle a_{v,k} a_{v,k}^\dagger \rangle; \quad (6)$$

As is well known, the dynamics of f_k does not yield a closed set of equations since both the Coulomb and phonon interaction Hamiltonians lead to coupling of the two-point quantities to either four-point quantities or mixed carrier-phonon operators. Schematically, the hierarchy problem^{1,20} is described by

$$i\hbar \frac{\partial}{\partial t} \langle N \rangle = T \langle N \rangle + V \langle N + 1 \rangle \quad (7)$$

where an N -particle (i.e. $2N$ -point) operator is coupled to $(N+1)$ -particle operators due to the many-body interaction. To solve this hierarchy problem rigorously, we apply a method known from quantum chemistry where the truncation problem for many-electron wave functions has successfully been approached with the so-called cluster expansion.^{21,22,23} There, the electronic wave function is divided into classes where electrons are: i) independent single particles (singlets), ii) coupled in pairs (doublets), iii) coupled in triplets, and iv) coupled in higher order clusters. The N -particle wave function is then approximated by a suitable amount of coupled clusters by including the correct antisymmetry of the fermions.

In semiconductors, the system properties can be evaluated from $2N$ -point expectation values $\langle N \rangle$ $a_{1,k_1}^\dagger a_{N,k_N}^\dagger a_{N,p_N} a_{1,p_1}$, which determine the reduced density matrix in the Bloch basis. If the system contains exactly N particles, $\langle N \rangle$ fully describes the system properties. In this case, $2N$ -point expectation values exist for all $N \geq 1$. The simplest approximation scheme is provided by the Hartree-Fock approximation which implicitly assumes that the many-body system is described by a so-called Slater determinant of N independent single-particle wave functions. In this case, $2N$ -point expectation values can be expressed in terms of two-point expectation values. For example, a four-point expectation value in singlet (i.e. Hartree-Fock) approximation is given by

$$\langle a_{1,k_1}^\dagger a_{2,k_2}^\dagger a_{2,p_2} a_{1,p_1} \rangle_S = \langle a_{1,k_1}^\dagger a_{1,p_1} \rangle \langle a_{2,k_2}^\dagger a_{2,p_2} \rangle - \langle a_{1,k_1}^\dagger a_{2,p_2} \rangle \langle a_{2,k_2}^\dagger a_{1,p_1} \rangle; \quad (8)$$

In the spirit of the original cluster expansion the system is thus fully described by uncorrelated singlets where each carrier behaves effectively like a single particle in a mean field of all other particles. Higher order contributions are defined recursively. For example, true two-particle correlations are obtained from

$$\langle a_{1,k_1}^\dagger a_{2,k_2}^\dagger a_{2,p_2} a_{1,p_1} \rangle = \langle a_{1,k_1}^\dagger a_{2,k_2}^\dagger a_{2,p_2} a_{1,p_1} \rangle_S - \langle a_{1,k_1}^\dagger a_{2,p_2} \rangle \langle a_{2,k_2}^\dagger a_{1,p_1} \rangle; \quad (9)$$

i.e., by subtracting the singlet contribution from the full expectation value. The advantage of this factorization is its direct physical interpretation. By subtracting the single-particle contribution, the resulting correlated part really describes the true two-particle correlations.^{24,25} In the same way, truly correlated triplets and higher clusters can be defined by subtracting all lower-level contributions.²⁶

If we only include plasma and pair-correlation effects in the analysis, an arbitrary N -particle expectation value can be expressed consistently with the singlet-doublet approximation $\langle N \rangle \approx \langle N \rangle_{SD}$. This determines uniquely how the truncation of the hierarchy has to be performed; we only need to solve dynamics of $\langle h \rangle$ and $\langle h^2 \rangle$ because any arbitrary $\langle N \rangle_{SD}$ consists only of two-point expectation values and four-point correlations. According to Eq. (7), we obtain

$$i\hbar \frac{\partial}{\partial t} \langle h \rangle = T_1[\langle h \rangle] + V_1[\langle h^2 \rangle] + V_1[\langle h^2 \rangle]; \quad (10)$$

$$i\hbar \frac{\partial}{\partial t} \langle h^2 \rangle = T_2[\langle h^2 \rangle] + V_2[\langle h^3 \rangle_{SD}]; \quad (11)$$

where $T_{1(2)}$ and $V_{1(2)}$ are known functionals defined by the specific form of the Heisenberg equation of motion. The consistent singlet-doublet-approximation is obtained when $\langle h^3 \rangle$ is approximated by $\langle h^3 \rangle_{SD}$; as a result, the infinite hierarchy is systematically truncated and Eqs. (10)-(11) are closed. In order to study exciton formation, we consequently have to know the exciton and carrier-carrier correlations

$$C_X^{q;k^0;k} = \langle a_{c;k}^y a_{v;k^0}^y a_{c;k^0+q} a_{v;k-q} \rangle; \quad (12)$$

$$C_e^{q;k^0;k} = \langle a_{c;k}^y a_{c;k^0}^y a_{c;k^0+q} a_{c;k-q} \rangle; \quad (13)$$

$$C_h^{q;k^0;k} = \langle a_{v;k}^y a_{v;k^0}^y a_{v;k^0+q} a_{v;k-q} \rangle; \quad (14)$$

in addition to the single-particle densities, Eq. (6).

In general, the $\langle N \rangle_{SD}$ truncation fully includes the (3) limit of the so-called dynamics controlled truncation scheme.^{27,28} Obviously, a similar relation holds as the number of clusters is increased; i.e. $(2N-1)$ is a subset of the N -particle cluster expansion. Furthermore, the cluster expansion can be used in regimes where (N) methods fail, e.g., when the exciting field is strong or the system becomes fully incoherent. When $\langle h^3 \rangle$ is approximated by including only the singlet part $\langle h^3 \rangle_S$ in Eq.(11), also the second Born approach³ is found to be a subset of the cluster expansion. Since in this case the doublet part is included only partially, the second Born scheme does not allow formation of bound states but rather describes microscopic scattering. This ideology can be directly generalized in order to include the triplets in the scattering level; for such an approach, the $\langle h^3 \rangle$ dynamics is solved but the resulting $\langle h^4 \rangle_{SDT}$ is approximated by $\langle h^4 \rangle_{SD}$. This simplifies the numerical complexity of the triplet terms considerably and allows their analytic evaluation on the scattering level.

The cluster expansion can also be used directly to classify and truncate carrier-phonon correlations using the formal equivalence between a boson operator and a pair of fermion operators. The operator equation of motion,

$$i\hbar \frac{\partial}{\partial t} D_{p;p_2}^{H_{phon} + H_P} = \langle D_{p;p_2} \rangle + \sum_{jk} G_{p;p_2} a_{jk}^y a_{jk+q}; \quad (15)$$

shows that one phonon operator is formally equivalent to a product of two electronic operators and that with every phonon absorption or emission process, an electron changes its momentum. In that sense, also the phonon interaction leads to an infinite hierarchy formally equivalent to the many-body hierarchy problem discussed above. For example,

$\langle D_{p;p_2} a_{jk}^y a_{jk+p} \rangle = \langle D_{p;p_2} a_{jk}^y a_{jk+p} \rangle - \langle D_{p;p_2} i\hbar a_{jk}^y a_{jk+p} \rangle$ describes correlations between carriers and phonons. A similar treatment of the quantized light-matter interaction has led to quantum-optical effects resulting, e.g., in squeezing and entanglement.^{16,29,30} The singlet-doublet truncation with a controlled scattering treatment of the triplets leads to a closed set of equations which includes the dominant correlations between lattice vibrations and carriers.

C. Coulomb Interaction

Since the Heisenberg equations of motion are linear with respect to the different parts of the total Hamiltonian (5), we examine these different parts separately. For the exciton correlations under the influence of Coulomb interaction, we obtain

$$i\hbar \frac{\partial}{\partial t} C_X^{q;k^0;k} = \langle C_X^{q;k^0;k} \rangle_{H_{kin} + H_C} = \langle C_X^{q;k^0;k} \rangle + \langle C_X^{q;k^0;k} \rangle_{H_C} = \langle C_X^{q;k^0;k} \rangle + \langle C_X^{q;k^0;k} \rangle_{H_C} \\ + V_{k-k^0-q} (1 - f_k^e) (1 - f_{k-q}^h) f_{k^0+q}^e f_{k^0}^h - f_k^e f_{k-q}^h (1 - f_{k^0+q}^e) (1 - f_{k^0}^h)$$

$$\begin{aligned}
& + V_{k-k^0-q} f_k^h f_{k^0}^h C_{e+X}^{q+k^0-l;l;k} + f_k^e f_{k^0+q}^e C_{h+X}^{q+k-l;k^0;l} \\
& + 1 f_k^e f_k^h V_{1k} C_X^{q;k^0;l} 1 f_{k^0+q}^e f_{k^0}^h V_{1k^0} C_X^{q;l;k} \\
& + f_k^h f_{k^0+q}^e V_{1q} C_X^{l;k^0;k} + f_k^e f_{k^0}^h V_{1q} C_X^{l;q+k^0-l;k-q+1} \\
& + f_{k^0+q}^e f_k^e V_{1k} C_X^{q+k-l;k^0;l} + f_{k^0}^h f_k^h V_{1k^0} C_X^{q+k^0-l;l;k} ; \tag{16}
\end{aligned}$$

which is coupled both to carrier densities and to electron and hole correlations $C_{e(h)}^{q;k^0;k}$ via the terms $C_{e(h)+X}^{q;k^0;k} = C_{e(h)}^{q;k^0;k} + C_X^{q;k^0;k}$. The dynamics of these correlations is described by similar equations given in App. A.

The interpretation of Eq. (16) is straightforward; the first line gives the kinetic evolution of the four-point operator with the renormalized energies $\tilde{\epsilon}_k^{e(h)} = \epsilon_k^{e(h)} - \sum_{k^0} V_{k-k^0} f_{k^0}^{e(h)}$. The second line contains the factorized source term which initiates the creation of excitonic correlations as soon as electrons and holes are present. This singlet source is altered by the direct influence of the correlations in the third line. The remaining six Coulomb sums describe the different possibilities how two out of the four fermions in $\psi_a^\dagger \psi_a \psi_b^\dagger \psi_b$ can interact via the Coulomb interaction. These sums lead to the possibility to form bound excitons. The major contributions originate from the first two of the six sums which are multiplied by a phase space filling factor instead of a density difference and are thus appreciable even for low densities. All other sums vanish for low density but become important when the density is increased. They are a consequence of the indistinguishability of electrons and holes and correspond to Coulomb interaction between carriers formally "belonging" to two different excitons. Equations investigating exciton formation in the $(3) \rightarrow 1$ limit¹⁵ do neither contain these additional f -dependent contributions nor the singlet source.

In order to obtain a closed set of equations for the incoherent dynamics of the pure carrier system, we also have to derive the equation of motion for electron and hole densities. They are given by

$$\frac{\partial}{\partial t} f_k^e \Big|_{H_{kin} + H_C} = \frac{2}{h} \text{Im} \sum_{k^0;q} V_q C_e^{q;k^0;k} V_{k-q-k^0} C_X^{q;k^0;k^0} ; \tag{17}$$

$$\frac{\partial}{\partial t} f_k^h \Big|_{H_{kin} + H_C} = \frac{2}{h} \text{Im} \sum_{k^0;q} V_q C_h^{q;k^0;k} + \sum_{k^0;q} V_{k-q-k^0} C_X^{q;k;k^0} ; \tag{18}$$

and describe the influence of the correlations on the carrier distributions. Since all incoherent four-point correlations are treated exactly, this approach includes the microscopic carrier-carrier scattering beyond the second Born approach.³

D. Phonon Interaction

As a consequence of the Coulomb interaction, excitonic correlations can build up since the carriers of opposite charge are attracted towards each other. However, two particles cannot be bound without the assistance of a third object due to energy and momentum conservation. In a many-body system, any additional carrier can be this third object and compensate the energy gained by the bound-state formation. This process inevitably leads to heating of the remaining carrier system such that further formation gets more and more improbable. By a coupling to phonons the excess energy can be directed out of the many-body carrier system into the phonon reservoir. For simplicity, we assume that the phonon system is basically unperturbed by the carrier dynamics and solve the phonon dynamics using the steady state Markov approximation with the assumption of thermal occupation of the different phonon states. Working out the phonon contributions to the dynamic equations, we obtain in the singlet-doublet approximation

$$\frac{\partial}{\partial t} f_k^e \Big|_{H_P} = \frac{2}{h} \sum_p \text{Im} \epsilon_{k,p}^e ; \tag{19}$$

$$\frac{\partial}{\partial t} f_k^h \Big|_{H_P} = \frac{2}{h} \sum_p \text{Im} \epsilon_{k,p}^h ; \tag{20}$$

$$i\hbar \frac{\partial}{\partial t} C_X^{q;k^0;k} \Big|_{H_P;SD} = \epsilon_{k;k-q-k^0} f_{k^0}^h f_{k-q}^h - \epsilon_{k^0;k^0+q-k} f_k^e f_{k^0+q}^e ;$$

(21)

$$\begin{aligned} i\hbar \frac{\partial}{\partial t} C_{e, H_P; SD}^{q; k^0; k} &= \sum_{k, q, k^0} \left(f_{k, q}^e f_{k^0}^e + f_{k^0, q}^e f_{k^0+q}^e - f_{k^0+q}^e f_k^e \right. \\ &\quad \left. + f_{k^0, q}^e f_k^e - f_{k, q}^e + f_{k, q}^e f_{k^0}^e - f_{k^0+q}^e \right); \end{aligned} \quad (22)$$

$$\begin{aligned} i\hbar \frac{\partial}{\partial t} C_{h, H_P; SD}^{q; k^0; k} &= \sum_{k, q, k^0} \left(f_{k, q}^h f_{k^0}^h + f_{k^0, q}^h f_k^h - f_{k^0+q}^h f_k^h \right. \\ &\quad \left. + f_{k^0, q}^h f_k^h - f_{k, q}^h + f_{k, q}^h f_{k^0}^h - f_{k^0+q}^h \right); \end{aligned} \quad (23)$$

where we have defined the term

$$\begin{aligned} e_{kP} &= i \sum_{P?} \mathcal{G}_{P?} \int f_{kP}^e (1 - f_k^e) \left(N_{P?}^{PH} g(\mu_k^e - \mu_{kP}^e - h_{P?}) \right. \\ &\quad \left. + (N_{P?}^{PH} + 1) g(\mu_k^e - \mu_{kP}^e + h_{P?}) \right) \\ &\quad + i \sum_{P?} \mathcal{G}_{P?} \int f_{kP}^e (1 - f_k^e) \left(N_{P?}^{PH} g(\mu_k^e - \mu_{kP}^e + h_{P?}) \right. \\ &\quad \left. + (N_{P?}^{PH} + 1) g(\mu_k^e - \mu_{kP}^e - h_{P?}) \right) \\ &\quad + i \sum_{P?} \mathcal{G}_{P?} \int C_{e, P?}^{p; l; k} \\ &\quad \quad \quad \sum_{lP?} \left(g(\mu_{lP}^e - \mu_l^e + h_{P?}) - g(\mu_{lP}^e - \mu_l^e - h_{P?}) \right); \\ &\quad + i \sum_{P?} \mathcal{G}_{P?} \int C_{X, P?}^{k, P, l; l; k} \\ &\quad \quad \quad \sum_{lP?} \left(g(\mu_l^h - \mu_{lP}^h + h_{P?}) - g(\mu_l^h - \mu_{lP}^h - h_{P?}) \right); \end{aligned} \quad (24)$$

and a similar expression for h_{kP} with $g(\mu) = (\mu + i\Gamma/2)$. The derivation of Eqs. (19)-(24) is presented in App. B. After being inserted into Eqs. (19) and (20), the first four lines of Eq. (24) have a straight forward interpretation as scattering rates. They are the typical scattering equations with a balance between scattering into (lines one and two) and scattering out of (lines three and four) electron state k . In both cases, phonon absorption and emission processes are possible. Since emission can happen even without any phonons present, the respective terms are proportional to $N_{P?}^{PH} + 1$. The last two lines are due to phonon coupling to higher order correlations. Since both the carrier and the correlation dynamics in Eqs. (19)-(23) are determined by similar terms, the corresponding phonon effects result from the cooling of the carrier plasma.

The actual exciton formation dynamics is described in the six-point (triplet) level. The major contribution of these triplet correlations can be evaluated at the scattering level²⁵ in analogy to the second-Born approximation for four-point correlations which has successfully been used to describe microscopic Coulomb and phonon scattering.^{1,3} Physically, this approach provides scattering of excitons with a third object excluding the formation of bound three-particle clusters. As discussed in App. B, the resulting equations can be written as

$$\begin{aligned} i\hbar \frac{\partial}{\partial t} C_{X, H_P; T}^{q; k^0; k} &= \sum_{P} \left(\tilde{\gamma}_{k, qP}^h + \tilde{\gamma}_{k^0+qP}^e - (\tilde{\gamma}_{k^0P}^h) - (\tilde{\gamma}_{kP}^e) \right) C_X^{q; k^0; k} \\ &\quad + \sum_{P} \left(\tilde{\gamma}_{k, qP}^e - (\tilde{\gamma}_{k, qP}^h) \right) C_X^{q; k^0; P} \\ &\quad + \sum_{P} \left(\tilde{\gamma}_{k^0, k^0P}^h - (\tilde{\gamma}_{k^0+q, k^0P}^e) \right) C_X^{q; P; k} \\ &\quad + \sum_{P} \left((\tilde{\gamma}_{k, qP}^h - \tilde{\gamma}_{k, qP}^e) + (\tilde{\gamma}_{k^0+q, qP}^e - \tilde{\gamma}_{k^0, qP}^h) \right) C_X^{P; k^0; k} \\ &\quad + \sum_{P} \left(\tilde{\gamma}_{k^0P, q}^h + \tilde{\gamma}_{k, qP}^e - (\tilde{\gamma}_{X, P; k}^{p; k^0+q}) \right) \\ &\quad + \sum_{P} \left(\tilde{\gamma}_{k^0P, q}^h - (\tilde{\gamma}_{k, qP, q}^h) \right) C_X^{P; k^0+q, P; k} \end{aligned}$$

$$\sum_{\mathbf{p}} \frac{X}{k; \mathbf{q} \mathbf{p}} \left(\frac{e}{k^0 + \mathbf{q} \mathbf{p}} \right) C_X^{p; k^0; k \mathbf{q} + \mathbf{p}} ; \quad (25)$$

where \hat{f} and \hat{n} are defined according to

$$\begin{aligned} \hat{f}_{k\mathbf{p}}^e = & \sum_{\mathbf{p}'} \frac{X}{\mathbf{p}'} \hat{f}_{\mathbf{p}\mathbf{p}'}^2 \left(N_{\mathbf{p}\mathbf{p}'}^{PH} + 1 - \hat{f}_k^e \right) g(\hat{n}_k^e - \hat{n}_{k-\mathbf{p}}^e + \hat{n}_{\mathbf{p}\mathbf{p}'}^e) \\ & + (N_{\mathbf{p}\mathbf{p}'}^{PH} + \hat{f}_k^e) g(\hat{n}_k^e - \hat{n}_{k-\mathbf{p}}^e - \hat{n}_{\mathbf{p}\mathbf{p}'}^e) ; \end{aligned} \quad (26)$$

$$\begin{aligned} \hat{h}_{k\mathbf{p}} = & \sum_{\mathbf{p}'} \frac{X}{\mathbf{p}'} \hat{f}_{\mathbf{p}\mathbf{p}'}^2 \left(N_{\mathbf{p}\mathbf{p}'}^{PH} + \hat{f}_k^h \right) g(\hat{n}_k^h - \hat{n}_{k-\mathbf{p}}^h + \hat{n}_{\mathbf{p}\mathbf{p}'}^h) \\ & + (N_{\mathbf{p}\mathbf{p}'}^{PH} + 1 - \hat{f}_k^h) g(\hat{n}_k^h - \hat{n}_{k-\mathbf{p}}^h - \hat{n}_{\mathbf{p}\mathbf{p}'}^h) ; \end{aligned} \quad (27)$$

$$\begin{aligned} \tilde{\hat{f}}_{k\mathbf{p}}^e = & \sum_{\mathbf{p}'} \frac{X}{\mathbf{p}'} \hat{f}_{\mathbf{p}\mathbf{p}'}^2 \left(N_{\mathbf{p}\mathbf{p}'}^{PH} + \hat{f}_{k-\mathbf{p}}^e \right) g(\hat{n}_k^e - \hat{n}_{k-\mathbf{p}}^e + \hat{n}_{\mathbf{p}\mathbf{p}'}^e) \\ & + (N_{\mathbf{p}\mathbf{p}'}^{PH} + 1 - \hat{f}_{k-\mathbf{p}}^e) g(\hat{n}_k^e - \hat{n}_{k-\mathbf{p}}^e - \hat{n}_{\mathbf{p}\mathbf{p}'}^e) ; \end{aligned} \quad (28)$$

$$\begin{aligned} \hat{h}_{k\mathbf{p}} = & \sum_{\mathbf{p}'} \frac{X}{\mathbf{p}'} \hat{f}_{\mathbf{p}\mathbf{p}'}^2 \left(N_{\mathbf{p}\mathbf{p}'}^{PH} + 1 - \hat{f}_{k-\mathbf{p}}^h \right) g(\hat{n}_k^h - \hat{n}_{k-\mathbf{p}}^h + \hat{n}_{\mathbf{p}\mathbf{p}'}^h) \\ & + (N_{\mathbf{p}\mathbf{p}'}^{PH} + \hat{f}_{k-\mathbf{p}}^h) g(\hat{n}_k^h - \hat{n}_{k-\mathbf{p}}^h - \hat{n}_{\mathbf{p}\mathbf{p}'}^h) ; \end{aligned} \quad (29)$$

Similar equations for electron and hole correlations are also given in App. B.

These six-point phonon scattering contributions lead to microscopic dephasing of correlations and we find the conservation law

$$4 \frac{\partial}{\partial t} \sum_{\mathbf{k}; k^0; \mathbf{q}} \frac{X}{\mathbf{H} \mathbf{p}} C_X^{q; k^0; k \mathbf{q} + \mathbf{p}} = 0 \quad (30)$$

for the complex valued correlations $C_X^{q; k^0; k}$ such that the phonon scattering has a dissipative character. This property allows formation as well as equilibration of correlations.

The set of equations (16)-(18), (A1), and (A2), extended by the phonon contributions, Eqs. (19)-(25), (B7) and (B8), provides a closed system of coupled differential equations which can be solved under different initial conditions in order to study exciton formation for different carrier densities and lattice temperatures.

III. EXCITON FORMATION

Because of the high dimensionality of the summations in our hierarchy of coupled equations, the currently available computer resources limit us to evaluate the equations for a one-dimensional model system. However, we choose parameters to be close to the standard GaAs parameters used for quantum wells. The effective width of our quantum wire is determined such that the exciton binding energy lies roughly 11 meV below the unrenormalized bandgap which is also the case in typical 8 nm quantum wells. The corresponding 3D-exciton Bohr radius is $a_0 = 12.4$ nm. To incorporate Coulomb screening effects to the four-point terms, we use a statically screened Coulomb potential obtained from the Lindhard formula.¹ Microscopically, the justification follows from the coupling to the six-point terms. For the carrier densities, the coupling to the doublet level provides a microscopic description of scattering and screening such that the unscreened matrix element is used in Eq. (17) and (18). In all calculations, we start from an incoherent electron-hole plasma with vanishing correlated doublets.

A. Direct Evidence of Exciton Formation

The formation of any significant amount of bound excitons can be directly observed via the electron-hole pair-correlation function^{24,31}

$$g^{eh}(\mathbf{r}) = \frac{1}{n^2} h_e^y(\mathbf{r}) h_h^y(0) - h_h(0) h_e(\mathbf{r}) i; \quad (31)$$

which is normalized with respect to the single-particle carrier density n and measures the conditional probability to find an electron at position \mathbf{r} while the hole is located at $\mathbf{r} = 0$. The pair-correlation function can be separated into

a singlet and a correlated doublet part

$$g^{\text{eh}}(r) = \frac{1}{(nL)^2} \sum_{\mathbf{k}; \mathbf{k}^0; \mathbf{p}; \mathbf{p}^0} e^{i(\mathbf{k} - \mathbf{k}^0) \cdot \mathbf{r}} h_{\mathbf{k}}^y a_{\mathbf{k}^0} v_{\mathbf{p}}^y v_{\mathbf{p}^0}^y = g_s^{\text{eh}}(r) + g^{\text{eh}}(r; t); \quad (32)$$

$$g_s^{\text{eh}}(r) = 1 + \frac{1}{nL} \sum_{\mathbf{k}} e^{i\mathbf{k} \cdot \mathbf{r}} P_{\mathbf{k}}^2; \quad (33)$$

$$g^{\text{eh}}(r) = \frac{1}{(nL)^2} \sum_{\mathbf{k}; \mathbf{k}^0; \mathbf{q}} e^{i(\mathbf{k} - \mathbf{k}^0 - \mathbf{q}) \cdot \mathbf{r}} C_X^{\mathbf{q}; \mathbf{k}^0; \mathbf{k}}; \quad (34)$$

where $P_{\mathbf{k}} = h a_{\mathbf{v}; \mathbf{k}}^y a_{\mathbf{c}; \mathbf{k}}^y$ is the coherent microscopic interband transition amplitude which provides the dominant contribution to the pair-correlation function after a coherent excitation with a classical field.³² As soon as this polarization dephases, however, the factorized contribution becomes constant and the only r -dependence is provided by the correlated part $g^{\text{eh}}(r)$. This quantity provides an intuitive measure of when and how fast exciton formation and ionization takes place in incoherent configurations.

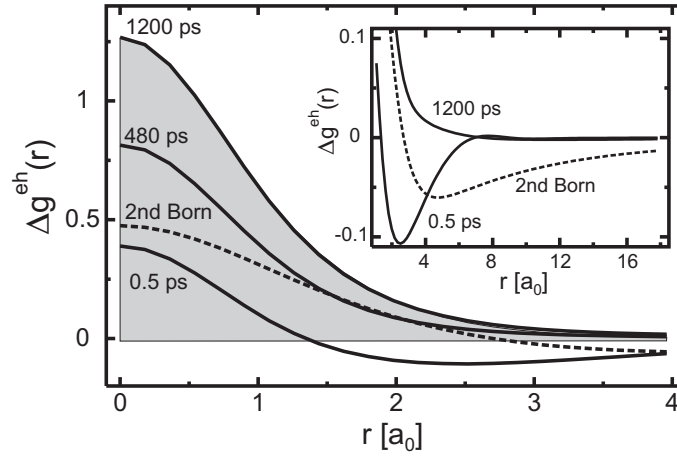


FIG. 1: Pair-correlation function $g^{\text{eh}}(r) = \langle n^{\text{eh}} \rangle$ normalized to the constant Hartree-Fock value for a lattice temperature of $T = 10\text{ K}$ and a carrier density of $n = 2 \cdot 10^4 \text{ cm}^{-3}$ at different times. For comparison, the wave function of the lowest bound exciton is given as a shaded area. The dashed line is the corresponding result of a second-Born computation. The inset shows a magnification of the tails of the same curves.

Figure 1 shows computed examples of $g^{\text{eh}}(r)$ as a function of electron-hole distance r for a low carrier density of $n^{\text{eh}} = 2 \cdot 10^4 \text{ cm}^{-3}$. At early times after the completely uncorrelated initialization of the system, the carriers react to the Coulomb attraction and the probability of finding electrons and holes close to each other increases. However, the correlated g^{eh} has clearly negative parts. At certain distances, the total pair correlation $g^{\text{eh}}(r)$ is therefore below its factorized value. We interpret this behavior as a fast rearrangement of the electron-hole plasma where the probability to find electrons in the close vicinity of holes is increased at the expense of the probability at around 2 to 4 a_0 . Since the area under g^{eh} provides a measure of how many excitons have formed²⁴, the early time dynamics does not show a real formation of excitons out of the plasma. Nevertheless, at 480 ps, the pair correlation has assumed the shape of an exciton relative-motion wave function (given as a shaded area) and grows almost linearly in time.

For comparison, we also show the second-Born result in Fig. 1 as a dashed line. In this approximation, the Coulomb sums of Eqs. (16) and the triplet phonon scattering, Eq. (25), are not included such that the doublets can describe only carrier-carrier scattering but not bound excitons. We see that the resulting pair-correlation function has similar characteristics as the early time g^{eh} in the full computation. In particular, g^{eh} drops to negative values before it approaches zero at large distances. Since no exciton populations are included in the second-Born computation, the resulting shape of the pair correlation has to be interpreted as a rearrangement within the plasma.

B. Phonon Induced Energy Transfer in Exciton Formation

Since a bound exciton at rest has a lower energy than a free electron-hole pair, we study the energy transfer during the exciton formation in the many-body system. For carriers alone, the system energy is

$$\begin{aligned} \hbar H_{kin} + \hbar H_C &= \sum_{\mathbf{k}} \hbar \mathbf{a}_{\mathbf{k}}^\dagger \mathbf{a}_{\mathbf{k}} + \frac{1}{2} \sum_{\mathbf{k}, \mathbf{k}^0, \mathbf{q} \in 0} V_{\mathbf{q}} \mathbf{a}_{\mathbf{k}}^\dagger \mathbf{a}_{\mathbf{k}^0}^\dagger \mathbf{a}_{\mathbf{k}^0 + \mathbf{q}} \mathbf{a}_{\mathbf{k}} \\ &= \hbar H_{kin}^e + \hbar H_{kin}^h + \hbar H_C^e + \hbar H_C^h \\ &\quad + \hbar H_C^e + \hbar H_C^h + \hbar H_C^{eh} \end{aligned} \quad (35)$$

with the kinetic energies $\hbar H_{kin} = \sum_{\mathbf{k}} \hbar \mathbf{f}_{\mathbf{k}}$, the incoherent singlet (factorized) parts to the Coulomb energy $\hbar H_C^e = \frac{1}{2} \sum_{\mathbf{k}, \mathbf{k}^0 \in 0} V_{\mathbf{k}} \mathbf{f}_{\mathbf{k}^0} \mathbf{f}_{\mathbf{k}}$, and the correlated contributions $\hbar H_C^h = \frac{1}{2} \sum_{\mathbf{k}, \mathbf{k}^0, \mathbf{q} \in 0} V_{\mathbf{q}} C_{\mathbf{X}}^{q, \mathbf{k}^0, \mathbf{k}}$ and $\hbar H_C^{eh} = \sum_{\mathbf{k}, \mathbf{k}^0, \mathbf{q} \in 0} V_{\mathbf{q}} C_{\mathbf{X}}^{k, \mathbf{q}, \mathbf{k}^0, \mathbf{k}}$. Using Eqs. (16)–(18) we find

$$\frac{\partial}{\partial t} [\hbar H_{kin} + \hbar H_C]_{\hbar H_{kin} + \hbar H_C} = 0 \quad (36)$$

which shows that the energy is conserved within the isolated carrier system. As a result, exciton formation is not efficient for a plain carrier system. When also phonons are included, we find

$$\frac{\partial}{\partial t} \hbar H_{tot} = \frac{\partial}{\partial t} [\hbar H_{kin} + \hbar H_C + \hbar H_{phon} + \hbar H_P] = 0; \quad (37)$$

i.e., the truncation via the cluster expansion scheme fully conserves the total energy of the system. When the phonons are included, the carrier system can cool down because part of the energy gained via exciton formation is transferred to lattice vibrations. When the phonons are treated as a reservoir, the phonon bath acts as a sink and the energy flux directed to the phonon system is absorbed by the reservoir. However, when we replace the microscopic phonon scattering, Eq. (25), by a simplified constant dephasing rate, we find

$$\frac{\partial}{\partial t} \hbar H_{tot} = \hbar H_C > 0 \quad (38)$$

which implies an unphysical heating of the system. Therefore, systematic exciton formation studies require a microscopic description of phonon scattering.

The dynamic evolution of the carrier energy is shown in Fig. 2 by using either constant dephasing or microscopic phonon scattering. With constant, the attractive Coulomb energy very quickly reaches its steady state value such that significant pair formation is not observed. Even a small constant of 50 eV leads to a linear heating of the carrier distributions, i.e., to an increase of the total energy. With the microscopic phonon scattering and a lattice temperature of 10 K, however, true formation of excitons is possible as indicated by the continuous decrease of the Coulomb energy. Simultaneously, the total energy of the carrier system decreases since part of the energy is lost to the phonon bath. The slope of decrease of the attractive Coulomb energy can in principle be used as a measure of how fast the exciton formation takes place.

To speed up the numerics, we have computed Fig. 2 by following the dynamics upto 40 ps with a phonon matrix-element enhanced by a factor of 30; this corresponds to 30 · 40 ps = 12 ns of formation dynamics. To verify the validity of this analysis we show in Fig. 3 a comparison for three enhancement factors of 10, 15, and 30. After rescaling the time axis with the respective factor, the behavior of the correlated Coulomb energy is indeed independent of the enhancement factor. In particular, the rate of change is very similar for all three cases which justifies the use of the artificial enhancement factors in the numerical investigations.

C. Formation of Specific Excitons

In the equation for excitonic correlations Eq. (16), two of the six Coulomb sums are usually dominant; the terms multiplied by the phase space filling factor $1 - f^e - f^h$ provide a large contribution for all densities. Therefore, the restriction to these two dominant sums is often a very good approximation to the full result. The corresponding "main sum approximation" of Eq. (16) is

$$i\hbar \frac{\partial}{\partial t} C_X^{q, \mathbf{k}^0, \mathbf{k}} = (n_{\mathbf{k}^0 + \mathbf{q}}^e - n_{\mathbf{k} - \mathbf{q}}^h - n_{\mathbf{k}}^e + n_{\mathbf{k}^0}^h) C_X^{q, \mathbf{k}^0, \mathbf{k}}$$

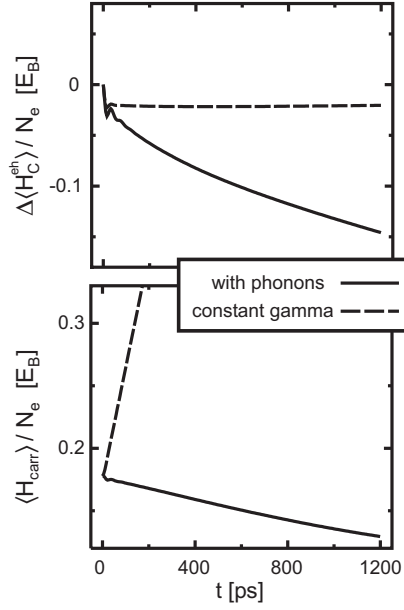


FIG. 2: Attractive Coulomb energy (a) and total energy (b) per particle comparing a computation with constant dephasing approximation (dashed line) with the full result including microscopic phonon scattering (solid line) for the same parameters as in Fig. 1. Energies are given in multiples of the 3D exciton binding energy $E_B = 42 \text{ meV}$.

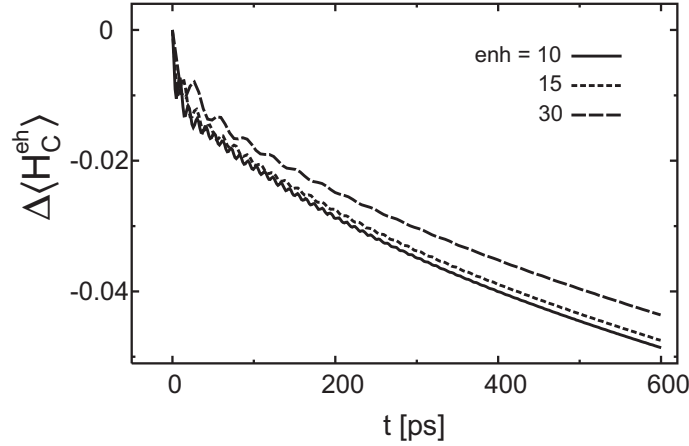


FIG. 3: Correlated Coulomb energy $\Delta\langle H_C^{eh} \rangle$ per particle for three different computations with different enhancement factors. For each curve, the time axis has been rescaled with the respective enhancement factor. The carrier density is $n = 1 \cdot 10^4 \text{ cm}^{-3}$ and the lattice temperature is $T = 10 \text{ K}$.

$$\begin{aligned}
 & + V_{k-k^0-q} \left((1 - f_k^e) (1 - f_{k-q}^h) f_{k^0+q}^e f_{k^0}^h - (1 - f_{k^0+q}^e) (1 - f_{k^0}^h) f_k^e f_{k-q}^h \right) \\
 & + \left[(1 - f_k^e) f_{k-q}^h - (1 - f_{k-q}^e) f_k^h \right] V_{1-k} C_X^{q;k^0;l} - \left[(1 - f_{k^0+q}^e) f_{k^0}^h - (1 - f_{k^0}^e) f_{k-q}^h \right] V_{1-k^0} C_X^{q;l;k} ;
 \end{aligned} \quad (39)$$

With this restriction, the excitonic correlations are not coupled to carrier-carrier correlations anymore and we obtain a closed subsystem of equations for each center-of-mass momentum q .

Since the carrier distributions typically vary slowly, we try to find an adiabatic solution for Eq. (39). To do so, we use a generalized exciton basis, which is defined by the equations

$$\mathbf{u}_{k;q}^r(k) = \left((1 - f_{k+q}^e) f_{k-q}^h \right)_{k^0} V_{k^0-k}^r(k^0) = E_{i;q}^r(k) ; \quad (40)$$

$$\mathbf{v}_{i;q}^r(k) = \mathbf{u}_{k;q}^r(k)_{k^0} - \left((1 - f_{k^0+q}^e) f_{k^0}^h \right) V_{k^0-k}^r(k^0) = \mathbf{v}_{i;q}^r(k) - E_{i;q}^r(k) ; \quad (41)$$

where we have defined $\mathbf{u}_{k;q} = \mathbf{u}_{k+q}^e + \mathbf{u}_{k-q}^h$ and $q^{e(h)} = q m_{e(h)} = (m_e + m_h)$. The main difference to the usual Wannier basis is that for non-zero densities the phase-space filling factor and a screened Coulomb potential enter the effective Hamiltonian. Therefore, the eigenvalue problem Eq. (40) is not Hermitian and one obtains left and right handed eigenfunctions $\psi_{i;q}^{(r)}$. This exciton basis fulfills a generalized orthogonality and completeness relation

$$\sum_{i;q} \psi_{i;q}^{(l)}(k) \psi_{0;q}^{(r)}(k) = \delta_{k,0}; \quad (42)$$

$$\sum_{i;q} \psi_{i;q}^{(l)}(k) \psi_{i;q}^{(r)}(k^0) = \delta_{k,k^0}; \quad (43)$$

The center-of-mass momentum q enters Eq. (40) via the phase-space filling factor such that the relative motion of an exciton depends also on its center-of-mass momentum.

By means of the generalized Wannier functions, one can introduce exciton annihilation operators

$$X_{i;q} = \sum_{k;q} \psi_{i;q}^{(l)}(k) v_{k-q}^y C_{k+q}^e; \quad (44)$$

$$v_{k-q}^y C_{k+q}^e = \sum_{i;q} \psi_{i;q}^{(r)}(k) X_{i;q} \quad (45)$$

and the Hermitian conjugate creation operators. Equations (44) and (45) can directly be applied to the correlations in order to transform them according to

$$C_X^{q;k^0,q^h;k+q^e} = \sum_{i;q} \psi_{i;q}^{(r)}(k) \psi_{0;q}^{(l)}(k^0) \langle X_{i;q}^y X_{0;q}^i \rangle; \quad (46)$$

$$\langle X_{i;q}^y X_{0;q}^i \rangle = \sum_{k;k^0} \psi_{i;q}^{(l)}(k) \psi_{0;q}^{(r)}(k^0) C_X^{q;k^0,q^h;k+q^e}; \quad (47)$$

This expansion cannot only be used to solve Eq. (39) but also to compute expectation values in the exciton basis from our numerical computations performed in the k -basis.

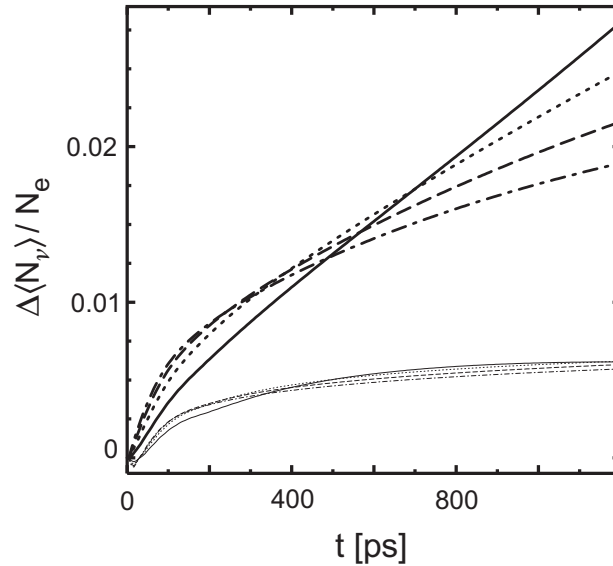


FIG. 4: Formation dynamics of q -integrated population correlations, Eq. (48), out of an electron-hole plasma with $n = 2 \cdot 10^4 \text{ cm}^{-3}$ at $T = 60 \text{ K}$. The lattice temperature was 10 K (solid line), 20 K (dotted line), 30 K (dashed line), and 40 K (dash-dotted line), respectively. Thick lines indicate $\langle N_{1s} \rangle$ whereas thin lines refer to $\langle N_{2p} \rangle$.

Using Eq. (47), we can study the formation of specific excitons as shown in Fig. 4. There, we have computed the dynamics for different lattice temperatures, always starting with initial electron and hole distributions at a temperature of $T = 60 \text{ K}$. With the help of Eq. (47), we compute the q -integrated exciton population correlations

$$\langle N_{1s} \rangle = \sum_q \langle N_{1s;q} \rangle = \sum_q \langle X_{1s;q}^y X_{1s;q}^i \rangle \quad (48)$$

normalized to the total number of electrons in the system. These populations as a function of time are shown for the two lowest bound excitons denoted 1s and 2p, respectively³⁴. Figure 4 clearly demonstrates how the formation rate of 1s excitons quickly drops for elevated lattice temperatures. For temperatures above 40 K, we do not expect any significant formation.

In order to continue our analytical derivation, we note that in the incoherent regime f^e and f^h typically change slowly such that the exciton wave functions $\chi_{\mathbf{q}}$ can be assumed to be quasistationary. With the help of this adiabatic approximation, Eq. (39) can be written as

$$i\hbar \frac{\partial}{\partial t} \langle \chi_{\mathbf{q}}^{\dagger} X_{\mathbf{0},\mathbf{q}} \rangle = (E_{\mathbf{0}} - E_{\mathbf{q}}) \langle \chi_{\mathbf{q}}^{\dagger} X_{\mathbf{0},\mathbf{q}} \rangle + \sum_{\mathbf{k};\mathbf{k}^0} \langle \chi_{\mathbf{q}}^{\dagger}(\mathbf{k}) \chi_{\mathbf{0},\mathbf{q}}(\mathbf{k}^0) \rangle S^{\mathbf{q};\mathbf{k}^0;\mathbf{k}} \quad (49)$$

with the factorized (singlet) source term

$$S^{\mathbf{q};\mathbf{k}^0;\mathbf{k}} = V_{\mathbf{k}-\mathbf{k}^0} \left(1 - f_{\mathbf{k}+\mathbf{q}}^e - f_{\mathbf{k}-\mathbf{q}}^h \right) f_{\mathbf{k}^0+\mathbf{q}}^e f_{\mathbf{k}^0-\mathbf{q}}^h - \left(1 - f_{\mathbf{k}^0+\mathbf{q}}^e - f_{\mathbf{k}^0-\mathbf{q}}^h \right) f_{\mathbf{k}+\mathbf{q}}^e f_{\mathbf{k}-\mathbf{q}}^h : \quad (50)$$

The properties of the left-handed exciton basis, Eq. (41), can be used to simplify the last term in Eq. (49) according to

$$\sum_{\mathbf{k};\mathbf{k}^0} \langle \chi_{\mathbf{q}}^{\dagger}(\mathbf{k}) \chi_{\mathbf{0},\mathbf{q}}(\mathbf{k}^0) \rangle S^{\mathbf{q};\mathbf{k}^0;\mathbf{k}} = (E_{\mathbf{0}} - E_{\mathbf{q}}) \langle \chi_{\mathbf{q}}^{\dagger} X_{\mathbf{0},\mathbf{q}} \rangle_{\text{IS}}; \quad (51)$$

where the factorized plasma part of the two-particle correlation is given by

$$\langle \chi_{\mathbf{q}}^{\dagger} X_{\mathbf{0},\mathbf{q}} \rangle_{\text{IS}} = \sum_{\mathbf{k}} \langle \chi_{\mathbf{q}}^{\dagger}(\mathbf{k}) \chi_{\mathbf{0},\mathbf{q}}(\mathbf{k}) \rangle f_{\mathbf{k}+\mathbf{q}}^e f_{\mathbf{k}-\mathbf{q}}^h : \quad (52)$$

In the exciton basis, the full equation is therefore

$$i\hbar \frac{\partial}{\partial t} \langle \chi_{\mathbf{q}}^{\dagger} X_{\mathbf{0},\mathbf{q}} \rangle = (E_{\mathbf{0}} - E_{\mathbf{q}}) \langle \chi_{\mathbf{q}}^{\dagger} X_{\mathbf{0},\mathbf{q}} \rangle + (E_{\mathbf{0}} - E_{\mathbf{q}}) \langle \chi_{\mathbf{q}}^{\dagger} X_{\mathbf{0},\mathbf{q}} \rangle_{\text{IS}} + i\hbar \frac{\partial}{\partial t} \langle \chi_{\mathbf{q}}^{\dagger} X_{\mathbf{0},\mathbf{q}} \rangle_{\text{T-scatt}} \quad (53)$$

where we have included the scattering contributions from triplet correlations.

The simple form of Eq. (53) reveals how the exciton formation proceeds. If we start the calculations assuming initially vanishing correlations, they start to build up because the source term $\langle \chi_{\mathbf{q}}^{\dagger} X_{\mathbf{0},\mathbf{q}} \rangle_{\text{IS}}$ is non-vanishing as soon as carriers are present in the system. However, that source term does not create diagonal correlations such that excitonic populations $\langle \chi_{\mathbf{q}} \rangle$ stay zero without the six-point scattering contribution. Hence, the formation of exciton populations in the incoherent regime has only one possible Coulombic channel where off-diagonal transition correlations $\langle \chi_{\mathbf{q}}^{\dagger} X_{\mathbf{0},\mathbf{q}} \rangle$ are created first. Only after off-diagonal transitions have been created, populations can be formed via the triplet scattering. Therefore, it is crucial to include both excitonic transition and population correlations in the formation analysis, as is done automatically in the full \mathbf{k} -basis treatment used in all our computations. If one uses excitonic models which are restricted to the diagonal populations, the formation channel via the transition correlations is completely omitted.

The efficiency and the character of the indirect exciton formation channel are analyzed in Fig. 5 which investigates the build-up of the integrated exciton population correlation $\langle \chi_{1s} \rangle$. Here, we compare a run where all off-diagonal transition correlations $\langle \chi_{\mathbf{q}}^{\dagger} X_{\mathbf{0},\mathbf{q}} \rangle$ are set to zero during the computation with a reference run without reset. For the reset, all correlations are transformed from the \mathbf{k} -basis into the exciton basis via Eq. (47) and back to the \mathbf{k} -basis with the help of Eq. (46). In the back transformation, we omit all but the diagonal correlations. No phonon-enhancement factor was used in this computation because we want to investigate Coulomb and phonon dynamics for equally short time scales. Exactly at the moment where the off-diagonal correlations are reset, the formation dynamics stops and no more exciton correlations can build up. On the contrary, the amount of 1s populations is even slightly decreased since the phonon scattering tends to transfer some of the diagonal populations back to off-diagonal transition correlations. Already around 3 ps after the reset, however, the off-diagonal transition correlations are fully recovered. After some transient dynamics, the formation continues with the previous formation rate. Also

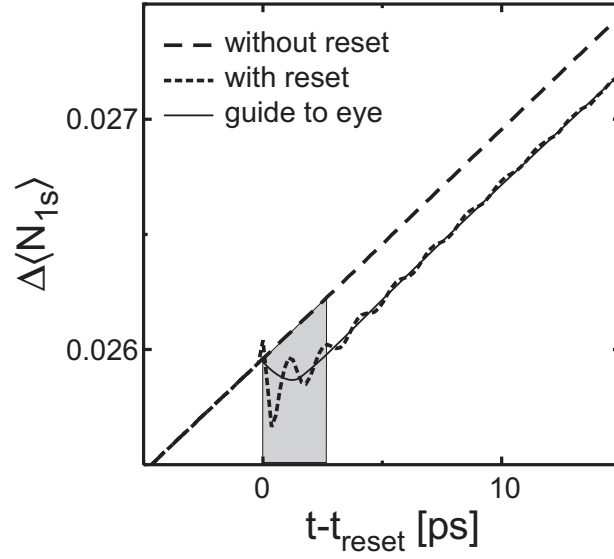


FIG. 5: Total exciton population correlation $\Delta \langle N_{1s} \rangle$ for two computations with (dotted) and without (dashed) reset of off-diagonal transition correlations for $n = 2 \times 10^{14} \text{ cm}^{-3}$ and $T = 10 \text{ K}$. The thin solid line is given as guide to the eye.

in other quantities, as for example in the correlated Coulomb energy, this fast recovery of the transition correlations is confirmed. This behavior indicates that off-diagonal transition correlations build up extremely quickly compared to the formation rate of diagonal populations. It is these off-diagonal transition correlations which cause the plasma like shape of the early-time pair-correlation function.

The importance of the off-diagonal exciton transitions can also be seen in the equation of motion of the electron density. By expressing the right hand side of Eq. (17) with the help of Eq. (46), we obtain

$$\frac{\partial f_k^e}{\partial t} \Big|_{\text{X corr}} = \sum_{q,q'} (E_{0,q} - E_{q,q'}) (v_{0,q}(k - q^e)) v_{q,q'}(k - q^e) \langle X_{q,q'}^y X_{0,q'}^x \rangle; \quad (54)$$

Thus, diagonal exciton populations do not change the carrier densities. Excitonic transitions are required in order to describe the full dynamics and the correct heating of the carrier plasma due to exciton formation.

D. Transition Correlations

In order to understand the general nature of the off-diagonal transition correlations, it is sufficient to investigate Eq. (53) where the six-point scattering contributions are approximated by a constant dephasing rate, i.e.,

$$\hbar \frac{\partial}{\partial t} \langle X_{q,q'}^y X_{0,q'}^x \rangle \Big|_{\text{T scatt}} = -\langle X_{q,q'}^y X_{0,q'}^x \rangle; \quad (55)$$

Since this term leads to a simple decay, Eq. (53) has a steady-state solution

$$\langle X_{q,q'}^y X_{0,q'}^x \rangle_{\text{steady state}} = \frac{E_{0,q} - E_{q,q'}}{E_{0,q} - E_{q,q'} - i} \langle X_{q,q'}^y X_{0,q'}^x \rangle_S; \quad (56)$$

For sufficiently small ϵ , we find

$$\langle X_{q,q'}^y X_{0,q'}^x \rangle = (\epsilon_{0,q} - 1) \langle X_{q,q'}^y X_{0,q'}^x \rangle_S; \quad (57)$$

For $\epsilon \rightarrow 0$, the off-diagonal correlations $\langle X_{q,q'}^y X_{0,q'}^x \rangle = \langle X_{q,q'}^y X_{0,q'}^x \rangle_S$ fully cancel with the singlet (two-point) contribution when the total $\langle X_{q,q'}^y X_{0,q'}^x \rangle$ is evaluated. The diagonal part $\langle X_{q,q'}^y X_{q,q'}^x \rangle$, however, is determined by the singlet contribution alone. In other words, we find

$$\langle X_{q,q'}^y X_{0,q'}^x \rangle; \quad \langle X_{q,q'}^y X_{q,q'}^x \rangle_S = \sum_k v_{q,q'}^1(k) f_{k+q^e}^e f_{k-q^h}^h; \quad (58)$$

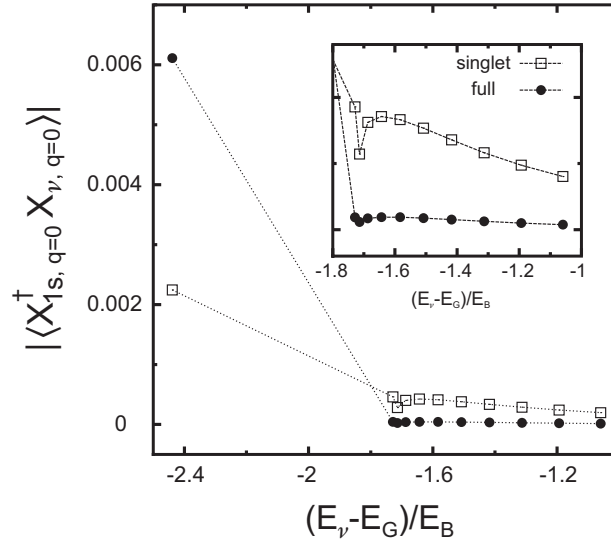


FIG. 6: Exciton correlations $\langle X_{1s,q=0}^\dagger X_{\nu,q=0} \rangle$ as function of energy E_ν after 720 ps of computation for the same parameters as in Fig. 1. The inset magnifies the region for energies higher than $E_G + 1.8E_B$. While off-diagonal correlations are largely reduced in the full computation, the diagonal exciton population increases in time due to genuine exciton formation.

where the solution is expressed with the help of Eq. (52).

Clearly, the off-diagonal transition correlations build up to compensate the off-diagonal two-point contributions whereas diagonal populations $\langle X_{\nu,q}^\dagger X_{\nu,q} \rangle$ have a non-vanishing and observable fermionic plasma contribution $\langle X_{\nu,q}^\dagger X_{\nu,q} \rangle_{\text{plasma}}$. These observations are valid also for the more general case where the six-point phonon scattering is included microscopically. Figure 6 shows the absolute value of the total exciton correlations $\langle X_{1s,q=0}^\dagger X_{\nu,q=0} \rangle$ as a function of the exciton energy E_ν for such a general calculation with microscopic phonon scattering. We compare the results of the full calculation with those obtained if we truncate the equations at the singlet level where no excitonic correlations are included.

The marker at the lowest energy gives the diagonal exciton population whereas the other markers indicate the magnitude of the respective off-diagonal transitions. We see, that a calculation at the singlet level predicts that the contributions of the off-diagonal transitions are quite appreciable (open squares) whereas the full calculation yields results that are more than an order of magnitude smaller (full circles). Hence, we find a high degree of cancellation between the singlet and the higher-order results as predicted by Eq. (58). Due to the very fast build-up of off-diagonal correlations compared to the slow phonon scattering, the steady-state result Eq. (57) for off-diagonal exciton transitions is still a good approximation for the full calculation. The main change to the simplified analysis leading to Eq. (58) is that under true formation conditions the diagonal exciton populations can grow and exceed their singlet contribution. Due to the formation dynamics, this diagonal population may increase in time and the difference to the plasma level determines the amount of true populations. This difference can also be seen in Fig. 6.

Even though the total correlations $\langle X_{\nu,q}^\dagger X_{\nu,q} \rangle$ are to a very good approximation diagonal in the exciton basis, the distinction between factorized and correlated part is very useful because the consistent theory shows that: i) only the truly correlated part of the off-diagonal exciton correlations leads to a significant contribution to the formation of excitons out of an incoherent plasma, ii) only the off-diagonal correlations influence the time evolution of the carrier distributions, and iii) even under good formation conditions, the correlated contribution to the exciton population is still of the same order of magnitude as its factorized counterpart. Both contributions certainly influence experiments and must be carefully distinguished. For example, the excitonic photoluminescence does not require the presence of true excitonic populations $\langle X_{\nu,q}^\dagger X_{\nu,q} \rangle$.³³

IV. SUMMARY

We have presented a general many-body formalism to describe the dynamics of charge carriers and two-particle correlations within semiconductor heterostructures. The Coulomb interaction between electrons and holes and the coupling of carriers and correlations to a phonon reservoir has been described microscopically. We thus are able to compute exciton formation times and exciton-exciton correlations without neglecting the underlying fermionic

properties. We have shown that the formation is an intricate process where Coulomb correlations rapidly build up on a picosecond time scale while phonon dynamics leads to true exciton formation on a slow nanosecond time scale. An adiabatic approximative solution has been obtained which provides an intuitive interpretation of the microscopic results.

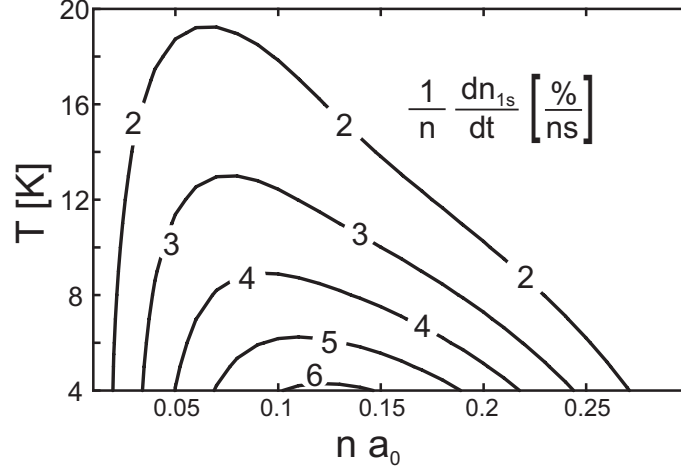


FIG. 7: Contour plot of exciton formation rates for an initial carrier temperature of 60 K and varying lattice temperatures and carrier densities. The exciton formation rates are taken at 1.2 ns of evolution and normalized by the carrier density. The contour lines thus determine which percentage of charge carriers are bound to 1s-excitons per nanosecond.

The basic results are summarized in Fig. 7. There, we show the exciton formation rate 1.2 ns after initialization of the computations. At this time, the formation proceeds almost linearly in time, c.f. Fig. 4, and the formation rate gives a good measure of the efficiency of the exciton formation. The contour lines show how many percent of electron-hole pairs are bound to 1s-excitons per nanosecond. Exciton formation is only efficient for cold lattice temperatures below 30 K and rather low densities. For too low densities, however, the rate of formation drops simply because it becomes increasingly improbable that electrons and holes find scattering partners necessary for the formation process.

Generally, we can interpret the formation of excitons as a build-up of correlations which does not change the number of electrons and holes in the system. An interpretation of excitons as atom-like entities only makes sense under very restricted conditions of a dilute gas where a small density of excitons interacts only very weakly with the remaining carriers. Under those conditions, our theory gives reasonable exciton numbers. Basically, the total number of excitons formed is controlled by the lifetime of the electron-hole excitations. In many realistic systems, this is in the order of ns because of non-radiative recombination at imperfections and/or impurities.

Acknowledgments

This work was supported by the Deutsche Forschungsgemeinschaft, by the Max-Planck research prize of the Humboldt Foundation and the Max-Planck Society, and by the Forschungszentrum Jülich with a CPU-time grant. M.K. acknowledges funding from the Swedish Natural Science Research Council (NFR) and the Goran Gustafssons Stiftelse and thanks the Center for Parallel Computers (PDC) to make their computer resources available for this project.

APPENDIX A: EQUATIONS FOR ELECTRON AND HOLE CORRELATIONS

In Section II C we have only presented the equation for the excitonic correlations $c_x^{qk^0;k}$. The remaining equations for electron-electron and hole-hole correlations are

$$\begin{aligned}
 i\hbar \frac{\partial}{\partial t} c_e^{qk^0;k} &= \hat{c}_k^e + \hat{c}_{k^0+q}^e - \hat{c}_k^e \hat{c}_k^e c_e^{qk^0;k} \\
 &+ V_{k-k^0-q} f_k^e f_{k^0+q}^e (1 - f_k^e) (1 - f_{k^0}^e) - f_k^e f_{k^0}^e - 1 - f_k^e q - 1 - f_{k^0+q}^e \\
 &- V_q f_k^e f_{k^0+q}^e (1 - f_k^e) (1 - f_{k^0}^e) - f_k^e f_{k^0}^e - 1 - f_k^e q - 1 - f_{k^0+q}^e
 \end{aligned}$$

$$\begin{aligned}
& + V_q \frac{f_{k^0+q}^e f_{k^0}^e}{f_{k^0+q}^e f_{k^0}^e} \frac{C_{e+X}^{k^0 q} l; l; k^0}{C_{e+X}^{q+k^0} l; l; k^0} \frac{f_k^e f_{k-q}^e}{f_k^e f_{k-q}^e} \frac{C_{e+X}^{q+k^0} l; l; k^0}{C_{e+X}^{q+k^0} l; l; k^0} \\
& + V_{k-k^0-q} \frac{f_{k^0+q}^e f_{k^0}^e}{f_{k^0+q}^e f_{k^0}^e} \frac{C_{e+X}^{k^0 q} l; l; k^0}{C_{e+X}^{q+k^0} l; l; k^0} \frac{f_k^e f_{k-q}^e}{f_k^e f_{k-q}^e} \frac{C_{e+X}^{q+k^0} l; l; k^0}{C_{e+X}^{q+k^0} l; l; k^0} \\
& + \frac{1}{V_{k-q}} \frac{f_{k^0+q}^e f_{k^0}^e}{f_{k^0+q}^e f_{k^0}^e} \frac{C_{e+X}^{k^0 q} l; l; k^0}{C_{e+X}^{q+k^0} l; l; k^0} \frac{f_k^e f_{k-q}^e}{f_k^e f_{k-q}^e} \frac{C_{e+X}^{q+k^0} l; l; k^0}{C_{e+X}^{q+k^0} l; l; k^0} \\
& + \frac{1}{V_{k-q}} \frac{f_{k^0+q}^e f_{k^0}^e}{f_{k^0+q}^e f_{k^0}^e} \frac{C_{e+X}^{k^0 q} l; l; k^0}{C_{e+X}^{q+k^0} l; l; k^0} \frac{f_k^e f_{k-q}^e}{f_k^e f_{k-q}^e} \frac{C_{e+X}^{q+k^0} l; l; k^0}{C_{e+X}^{q+k^0} l; l; k^0} \\
& + \frac{1}{V_{k-q}} \frac{f_{k^0+q}^e f_{k^0}^e}{f_{k^0+q}^e f_{k^0}^e} \frac{C_{e+X}^{k^0 q} l; l; k^0}{C_{e+X}^{q+k^0} l; l; k^0} \frac{f_k^e f_{k-q}^e}{f_k^e f_{k-q}^e} \frac{C_{e+X}^{q+k^0} l; l; k^0}{C_{e+X}^{q+k^0} l; l; k^0} ;
\end{aligned} \tag{A 1}$$

$$\begin{aligned}
& i\hbar \frac{\partial}{\partial t} C_{h+X}^{q; k^0; k} = \tilde{\gamma}_{k-q}^h \tilde{\gamma}_{k^0+q}^h + \tilde{\gamma}_{k^0}^h + \tilde{\gamma}_k^h C_{h+X}^{q; k^0; k} \\
& + V_{k-k^0-q} \frac{1}{V_{k-q}} \frac{f_{k^0+q}^h f_{k^0}^h}{f_{k^0+q}^h f_{k^0}^h} \frac{C_{h+X}^{k^0 q} l; l; k^0}{C_{h+X}^{q+k^0} l; l; k^0} \frac{f_k^h f_{k-q}^h}{f_k^h f_{k-q}^h} \frac{C_{h+X}^{q+k^0} l; l; k^0}{C_{h+X}^{q+k^0} l; l; k^0} \\
& + V_q \frac{1}{V_{k-q}} \frac{f_{k^0+q}^h f_{k^0}^h}{f_{k^0+q}^h f_{k^0}^h} \frac{C_{h+X}^{k^0 q} l; l; k^0}{C_{h+X}^{q+k^0} l; l; k^0} \frac{f_k^h f_{k-q}^h}{f_k^h f_{k-q}^h} \frac{C_{h+X}^{q+k^0} l; l; k^0}{C_{h+X}^{q+k^0} l; l; k^0} \\
& + V_{k-k^0-q} \frac{1}{V_{k-q}} \frac{f_{k^0+q}^h f_{k^0}^h}{f_{k^0+q}^h f_{k^0}^h} \frac{C_{h+X}^{k^0 q} l; l; k^0}{C_{h+X}^{q+k^0} l; l; k^0} \frac{f_k^h f_{k-q}^h}{f_k^h f_{k-q}^h} \frac{C_{h+X}^{q+k^0} l; l; k^0}{C_{h+X}^{q+k^0} l; l; k^0} \\
& + V_q \frac{1}{V_{k-q}} \frac{f_{k^0+q}^h f_{k^0}^h}{f_{k^0+q}^h f_{k^0}^h} \frac{C_{h+X}^{k^0 q} l; l; k^0}{C_{h+X}^{q+k^0} l; l; k^0} \frac{f_k^h f_{k-q}^h}{f_k^h f_{k-q}^h} \frac{C_{h+X}^{q+k^0} l; l; k^0}{C_{h+X}^{q+k^0} l; l; k^0} \\
& + V_{k-k^0-q} \frac{1}{V_{k-q}} \frac{f_{k^0+q}^h f_{k^0}^h}{f_{k^0+q}^h f_{k^0}^h} \frac{C_{h+X}^{k^0 q} l; l; k^0}{C_{h+X}^{q+k^0} l; l; k^0} \frac{f_k^h f_{k-q}^h}{f_k^h f_{k-q}^h} \frac{C_{h+X}^{q+k^0} l; l; k^0}{C_{h+X}^{q+k^0} l; l; k^0} \\
& + \frac{1}{V_{k-q}} \frac{f_{k^0+q}^h f_{k^0}^h}{f_{k^0+q}^h f_{k^0}^h} \frac{C_{h+X}^{k^0 q} l; l; k^0}{C_{h+X}^{q+k^0} l; l; k^0} \frac{f_k^h f_{k-q}^h}{f_k^h f_{k-q}^h} \frac{C_{h+X}^{q+k^0} l; l; k^0}{C_{h+X}^{q+k^0} l; l; k^0} :
\end{aligned} \tag{A 2}$$

APPENDIX B : PHONON INTERACTION

The general phonon interaction Hamiltonian Eq. (4) is the starting point to compute the operator equation of motion for a two-point operator

$$i\hbar \frac{\partial}{\partial t} a_{jk}^y a_{jk+q}^y = \sum_p G_p a_{jk}^y a_{jk+q-p}^y - a_{jk+p}^y a_{jk+q}^y ; \tag{B 1}$$

where the collective phonon operator

$$G_p = \sum_{p'} G_{p;p'} - D_{p;p'} + D_{p;p'}^y ; \tag{B 2}$$

has been defined. With the help of this operator equation, we can now generate all other equations of motion. The simplest case is the equation for carrier densities. For electrons, we obtain

$$i\hbar \frac{\partial}{\partial t} f_k^e = \sum_p \hbar G_p a_{c;k}^y a_{c;k-p}^y - \hbar c. \tag{B 3}$$

In order to compute the right-hand side of Eq. (B 3), we have to establish the equations of motion for the phonon assisted terms. In the case of the phonon assisted electron density, this gives

$$i\hbar \frac{\partial}{\partial t} \hbar D_{p;p'} a_{c;k}^y a_{c;k-p}^y = G_{p;p'} f_{k-p}^e (1 - f_k^e)$$

$$\begin{aligned}
& + \hbar D_{p;p'} \sum_{\mathbf{k}} G_p i (f_{\mathbf{k}}^e - f_{\mathbf{k}-\mathbf{p}}^e) \\
& + G_{p;p'} \sum_{\mathbf{k}} C_e^{p;k} C_X^{k-p} i; \quad (B4)
\end{aligned}$$

where we have already left out all terms proportional to the coherent transition amplitudes $P_k = \hbar v_k^y c_k i$. In cases with coherent excitations, those terms can easily be included. But since in this case the Coulomb scattering is usually dominant, the main application of the microscopic phonon scattering lies in the incoherent regime. In order to compute Eq. (B3), we solve Eq. (B4) in Markov approximation. In principle, the result of a Markov approximation is dependent on the basis which we use. In general, however, the difference is not crucial if the resulting terms are summed over as is the case in Eq. (B3). For the computations, we have therefore included only terms proportional to the square of the phonon matrix elements. No Coulomb or light-matter interaction was included in the equation of phonon-assisted densities. The Markov approximation was done in the one-particle basis of Bloch electrons and holes. We numerically confirmed that our result is independent of the precise choice of the basis. Additionally, we assume a reservoir of phonons, i.e., we neglect coherent phonons and set $\hbar D_{p;p'} D_{p;p'} i = (\exp(E_{p;p'} / (kT)))^{-1}$ to the Bose-Einstein distribution at the corresponding energy $E_{p;p'}$ given by the phonon dispersion. After those approximations, we obtain Eqs. (19) and (20) for the carrier densities.

We have seen in Sec. IID that Eq. (B4) and its counterpart for the phonon-assisted hole densities suffice to compute the doublet contributions to the correlation equations. In addition, phonon-assisted correlations of the form $\hbar D a^y a^y a a i$ were needed in order to provide a true dephasing mechanism for excitons and carrier-carrier correlations on the triplet level. More specifically, the phonon contribution to the equation of motion for excitonic correlations is

$$\begin{aligned}
& i\hbar \frac{\partial}{\partial t} \hbar a_{c;k}^y a_{v;k^0}^y a_{c;k^0+q} a_{v;k-q} i = \\
& \sum_{\mathbf{k}} \hbar G_{k^0+q,k}^y a_{c;k}^y a_{c;k^0+q} i f_{\mathbf{k}-q}^h - f_{\mathbf{k}^0}^h \sum_{\mathbf{k}} \hbar G_{k^0+q,k}^y a_{v;k^0}^y a_{v;k-q} i f_{\mathbf{k}}^e - f_{\mathbf{k}^0+q}^e \\
& + \sum_{\mathbf{k}} \hbar G_p^y a_{c;k}^y a_{v;k^0}^y a_{c;k^0+q} a_{v;k-q+p} i \sum_{\mathbf{k}} \hbar G_p^y a_{c;k-p}^y a_{v;k^0-p}^y a_{c;k^0+q} a_{v;k-q} i \\
& + \sum_p \hbar G_p^y a_{c;k}^y a_{v;k^0}^y a_{c;k^0+q+p} a_{v;k-q} i \sum_p \hbar G_p^y a_{c;k}^y a_{v;k^0-p}^y a_{c;k^0+q} a_{v;k-q} i \quad (B5)
\end{aligned}$$

and similar equations exist also for the carrier-carrier correlations. The first row involves the phonon-assisted densities solved already in Eq. (B4). The remaining phonon-assisted correlations are solved via

$$\begin{aligned}
& i\hbar \frac{\partial}{\partial t} \hbar D_{p;p'} a_{c;k}^y a_{v;k^0}^y a_{c;k^0+q} a_{v;k-q-p} i = \\
& G_{p;p'} \left(N_{p;p'}^{PH} + f_{\mathbf{k}-q-p}^h \right) \hbar a_{c;k}^y a_{v;k^0}^y a_{c;k^0+q} a_{v;k-q} i \\
& + G_{p;p'} \left(N_{p;p'}^{PH} + 1 - f_{\mathbf{k}^0+q}^e \right) \hbar a_{c;k}^y a_{v;k^0}^y a_{c;k^0+q+p} a_{v;k-q-p} i \\
& G_{p;p'} \left(N_{p;p'}^{PH} + 1 - f_{\mathbf{k}^0}^h \right) \hbar a_{c;k}^y a_{v;k^0-p}^y a_{c;k^0+q} a_{v;k-q-p} i \\
& G_{p;p'} \left(N_{p;p'}^{PH} + f_{\mathbf{k}}^e \right) \hbar a_{c;k-p}^y a_{v;k^0-p}^y a_{c;k^0+q} a_{v;k-q-p} i \quad (B6)
\end{aligned}$$

which together with similar terms for phonon-assisted carrier-carrier correlations can be used to build up the complete phonon interaction contributions to the correlation equations. Again, we have kept only incoherent terms which enter the correlation equations proportional to the square of the phonon matrix element. Equation (B6) is solved in Markov approximation assuming a phonon bath characterized by the lattice temperature. This way, we obtain Eq. (25) and the corresponding equations

$$\begin{aligned}
& i\hbar \frac{\partial}{\partial t} C_e^{q;k^0;k} = \sum_{\mathbf{p}} \left(\tilde{c}_{\mathbf{k}-q;p}^e + \tilde{c}_{\mathbf{k}^0+q;p}^e \right) (\tilde{c}_{\mathbf{k}^0;p}^e) (\tilde{c}_{\mathbf{k};p}^e) C_e^{q;k^0;k} \\
& \sum_{\mathbf{k}} \left(\tilde{c}_{\mathbf{k};k-p}^e \right) (\tilde{c}_{\mathbf{k}-q;k-p}^e) C_e^{q;k^0;p} \sum_{\mathbf{p}} \left(\tilde{c}_{\mathbf{k}^0;k^0-p}^e \right) (\tilde{c}_{\mathbf{k}^0+q;k^0-p}^e) C_e^{q;p;k} \\
& \sum_p \left(\tilde{c}_{\mathbf{k}-q;p-q}^e \right) + \left(\tilde{c}_{\mathbf{k}^0+q;q-p}^e \right) C_e^{p;k^0;k} + \sum_{\mathbf{k}} \left(\tilde{c}_{\mathbf{k}^0;p-q}^e + \tilde{c}_{\mathbf{k};q-p}^e \right) (C_e^{p;k-q;k^0+q}) \\
& \sum_p \left(\tilde{c}_{\mathbf{k}^0;p-q}^e \right) (\tilde{c}_{\mathbf{k}-q;p-q}^e) C_e^{p;k^0+q;p;k} \sum_p \left(\tilde{c}_{\mathbf{k};q-p}^e \right) (\tilde{c}_{\mathbf{k}^0+q;q-p}^e) C_e^{p;k^0;k-q+p} \quad (B7)
\end{aligned}$$

and

$$\begin{aligned}
 i\hbar \frac{\partial}{\partial t} C_h^{q;k^0;k} &= \sum_{p \in H \cup T} \tilde{C}_k^h + \tilde{C}_{k^0+q;p}^h - (\tilde{C}_{k^0;p}^h) - (\tilde{C}_{k;p}^h) C_h^{q;k^0;k} \\
 &+ \sum_{p \in H \cup T} \tilde{C}_{k;k}^h - (\tilde{C}_{k;q;k}^h) C_h^{q;k^0;p} + \sum_{p \in H \cup T} \tilde{C}_{k^0;k^0;p}^h - (\tilde{C}_{k^0+q;k^0;p}^h) C_h^{q;p;k} \\
 &+ \sum_{p \in H \cup T} (\tilde{C}_{k;q;p}^h) + (\tilde{C}_{k^0+q;p}^h) C_h^{p;k^0;k} + \sum_{p \in H \cup T} \tilde{C}_{k^0;p}^h + \tilde{C}_{k;q;p}^h (C_h^{p;k} - C_h^{q;k^0+q}) \\
 &+ \sum_{p \in H \cup T} \tilde{C}_{k^0;p}^h - (\tilde{C}_{k;q;p}^h) C_h^{p;k^0+q;p;k} + \sum_{p \in H \cup T} \tilde{C}_{k;q;p}^h - (\tilde{C}_{k^0+q;p}^h) C_h^{p;k^0;k} - q+p
 \end{aligned} \quad (B 8)$$

where the terms \tilde{C} and \sim are identical to those defined in Eqs. (26)–(29).

walter.hoyer@physik.uni-mainz.de

- ¹ H. H. Haug and S. W. Koch, *Quantum Theory of the Optical and Electronic Properties of Semiconductors* (World Scientific Publ., Singapore, 1994), 3rd ed.
- ² F. Jahnke, M. Kira, S. W. Koch, G. Khitrova, E. K. Lindmark, T. R. Nelson Jr., D. V. Wick, J. D. Berger, O. Lyngnes, H. M. Gibbs, et al., *Phys. Rev. Lett.* **77**, 5257 (1996).
- ³ F. Jahnke, M. Kira, and S. W. Koch, *Z. Physik B* **104**, 559 (1997).
- ⁴ P. Borri, W. Langbein, J. M. Hvam, and F. Martelli, *Phys. Rev. B* **59**, 2215 (1999).
- ⁵ B. Mieck, H. Haug, W. A. Hugel, M. F. Heinrich, and M. Wegener, *Phys. Rev. B* **62**, 2686 (2000).
- ⁶ F. Tassone, F. Bassani, and L. C. Andreani, *Phys. Rev. B* **45**, 6023 (1992).
- ⁷ L. C. Andreani, *Phys. Lett. A* **192**, 99 (1994).
- ⁸ G. Khitrova, H. M. Gibbs, F. Jahnke, M. Kira, and S. W. Koch, *Rev. Mod. Phys.* **71**, 1591 (1999).
- ⁹ T. Uchi, *Prog. Theor. Phys.* **23**, 787 (1960).
- ¹⁰ D. Snoke, J. P. Wolfe, and A. Mysyrowicz, *Phys. Rev. Lett.* **59**, 827 (1987).
- ¹¹ K. Johnson and G. M. Kavoulakis, *Phys. Rev. Lett.* **86**, 858 (2001).
- ¹² M. Gulia, F. Rossi, E. Molinari, P. E. Selmann, and P. H. Lugli, *Phys. Rev. B* **55**, 16049 (1997).
- ¹³ A. L. Ivanov, P. B. Littlewood, and H. Haug, *Phys. Rev. B* **59**, 5032 (1999).
- ¹⁴ A. Thranhardt, S. Kuckenburg, A. Knorr, T. Meier, and S. W. Koch, *Phys. Rev. B* **62**, 2706 (2000).
- ¹⁵ K. Siantidis, V. M. Axt, and T. Kuhn, *Phys. Rev. B* **65**, 035303 (2001).
- ¹⁶ M. Kira, F. Jahnke, W. Hoyer, and S. W. Koch, *Prog. in Quant. Electr.* **23**, 189 (1999).
- ¹⁷ J. Hader, P. Thomas, and S. W. Koch, *Prog. in Quant. Electr.* **22**, 123 (1998).
- ¹⁸ H. Haug and A.-P. Jauho, *Quantum Kinetics in Transport & Optics of Semiconductors* (Springer-Verlag, Berlin, 1996), 1st ed.
- ¹⁹ N. Ashcroft and N. Mermin, *Solid State Physics* (Saunders College Publishing, New York, 1976), 1st ed.
- ²⁰ W. Schafer and M. Wegener, *Semiconductor Optics and Transport Phenomena* (Springer-Verlag, Berlin, 2002), 1st ed.
- ²¹ J. Czek, *J. Chem. Phys.* **45**, 4256 (1966).
- ²² G. D. Purvis and R. J. Bartlett, *J. Chem. Phys.* **76**, 1910 (1982).
- ²³ F. E. Harris, H. J. Monkhorst, and D. L. Freeman, *Algebraic and Diagrammatic Methods in Many-Fermion Theory* (Oxford Press, New York, 1992), 1st ed.
- ²⁴ W. Hoyer, M. Kira, and S. W. Koch, *Phys. Stat. Sol. (b)* **234**, 195 (2002).
- ²⁵ M. Kira, W. Hoyer, and S. W. Koch, *Journal of Nonlinear Optics B* (2002), accepted.
- ²⁶ J. Fricke, *Annals of Physics* **252**, 479 (1996).
- ²⁷ M. Lindberg, Y. Z. Hu, R. Binder, and S. W. Koch, *Phys. Rev. B* **50**, 18060 (1994).
- ²⁸ V. M. Axt and A. Stahl, *Z. Phys. B* **93**, 195 (1994).
- ²⁹ Y.-S. Lee, T. B. Norris, M. Kira, F. Jahnke, S. W. Koch, G. Khitrova, and H. M. Gibbs, *Phys. Rev. Lett.* **83**, 5338 (1999).
- ³⁰ C. Ell, P. Brück, M. Hubner, E. S. Lee, O. Lyngnes, J. P. Prineas, G. Khitrova, H. M. Gibbs, M. Kira, F. Jahnke, et al., *Phys. Rev. Lett.* **85**, 5392 (2000).
- ³¹ R. Zimmernann, *Many-Particle Theory of Highly Excited Semiconductors* (Teubner Verlagsgesellschaft., Leipzig, 1988), 1st ed.
- ³² Q. T. Vu, H. Haug, and L. V. Keldysh, *Solid State Commun.* **115**, 63 (2000).
- ³³ M. Kira, F. Jahnke, and S. W. Koch, *Phys. Rev. Lett.* **81**, 3263 (1998).
- ³⁴ In a one-dimensional model system, all exciton wave functions have a defined parity and are either even or odd functions. In analogy to the common nomenclature, we label the bound states 1s, 2p, 3s, and so forth.